



## Epitaxial bilayer $\text{La}_{0.7}\text{Sr}_{0.3}\text{MnO}_3/\text{Ba}_{0.7}\text{Sr}_{0.3}\text{TiO}_3$ thin films obtained by polymer assisted deposition

Danica Piper<sup>1,\*</sup>, Jelena Vukmirovic<sup>1</sup>, Iva Tokovic<sup>1</sup>, Akos Kukovecz<sup>2</sup>, Imre Szenti<sup>2</sup>, Mirjana Novakovic<sup>3</sup>, Marija Milanovic<sup>1</sup>, Vladimir V. Srdic<sup>1,\*</sup>

<sup>1</sup>Department of Materials Engineering, Faculty of Technology, University of Novi Sad, Bul. Cara Lazara 1, 21000, Novi Sad, Serbia

<sup>2</sup>Department of Applied and Environmental Chemistry, University of Szeged, Rerrich B. ter 1. H-6720 Szeged, Hungary

<sup>3</sup>Department of Atomic Physics, Vinča Institute of Nuclear Sciences - National Institute of the Republic of Serbia, University of Belgrade, M. Petrovića Alasa 12-14, 11351, Vinča, Beograd, Serbia

Received 20 April 2023; Received in revised form 21 June 2023; Accepted 25 June 2023

### Abstract

In this work bilayer structures, composed of ferromagnetic manganite and ferroelectric titanate layers, were obtained by solution deposition technique. The first step in preparation of the bilayer thin films was deposition of manganite ( $\text{LaMnO}_3$  or  $\text{La}_{0.7}\text{Sr}_{0.3}\text{MnO}_3$ ) layer by water-based polymer assisted deposition (PAD). Polycrystalline structures were obtained when manganite films were deposited by spin coating on commercial Pt/TiO<sub>2</sub>/SiO<sub>2</sub>/Si type substrate, whereas epitaxial films were grown on a single crystal SrTiO<sub>3</sub> with (001) orientation substrate. The second ferroelectric titanate ( $\text{BaTiO}_3$  or  $\text{Ba}_{0.7}\text{Sr}_{0.3}\text{TiO}_3$ ) layer was deposited by spin coating using sol-gel method. The obtained bilayer structures have thickness below 100 nm, and epitaxial growth of the  $\text{Ba}_{0.7}\text{Sr}_{0.3}\text{TiO}_3$  film on the  $\text{La}_{0.7}\text{Sr}_{0.3}\text{MnO}_3$  surface was obtained, due to the similar lattice parameters between these two crystal structures.

**Keywords:**  $\text{La}_{0.7}\text{Sr}_{0.3}\text{MnO}_3$ ,  $\text{Ba}_{0.7}\text{Sr}_{0.3}\text{TiO}_3$ , epitaxial bilayer films, solution deposition, microstructure

### I. Introduction

A very attractive way to create novel structures is to combine materials with different physical properties in one single structure, thus, improving its final functionality. One group of such novel multifunctional materials is multiferroics [1–3], characterized with the coexistence of at least two ferroic orders (ferroelectric, ferromagnetic and ferroelastic). The coexistence of ferroelectricity and ferromagnetism and a strong coupling interaction between the two ferroic orders (defined as magnetoelectric effect) is the most important factor for new applications in multifunctional devices [4,5]. In addition, interaction between spins and light, as well as optical control of magnetism at the nanoscale, is the main focus of recent fundamental studies of magnetism [6].

The attractiveness of  $\text{LaMnO}_3$  based materials has been growing over time due to their exceptional magnetoelectric properties [7,8]. Their structure and properties can be relatively easily manipulated by doping (for example with  $\text{Sr}^{2+}$ ,  $\text{Ca}^{2+}$ , etc.) and corresponding epitaxial thin films become important for application in spintronics and data storage devices. Several investigations based on multiferroic bilayer thin films having  $\text{LaMnO}_3$  based structures have been reported in literature showing very interesting magnetoelectric properties [9–13]. These heterostructures possess large interaction area and remarkable tunability between ferroelectric and magnetic order parameters which opens a new field of research and offers new possibilities.

Production of high-quality doped  $\text{LaMnO}_3$  thin films is usually based on expensive and complicated vapour deposition techniques [14]. However, recently chemical solution deposition (CSD) techniques were also under consideration due to their simplicity, low cost and

\*Corresponding author: tel: +381 21 450 3665  
e-mail: [dana.piper24@gmail.com](mailto:dana.piper24@gmail.com) (Danica Piper)  
[srdicvv@uns.ac.rs](mailto:srdicvv@uns.ac.rs) (Vladimir V. Srdic)

ability for large-scale production. Sol-gel is perhaps the most well-known and extensively studied CSD method, but there are also techniques such as citrate method, chemical bath deposition, metal organic deposition etc. [15]. Recently, polymer assisted deposition (PAD) has also been developed for deposition of simple and complex epitaxial metal-oxide films with desired structure and properties [16–18]. In PAD technique, aqueous solution of metal cations together with the corresponding polymers are used to form covalent complexes with metal cations and thus deactivate them while in solution [18]. The association of metal ions with polymers prevents the nucleation of the metal-oxide phase until depolymerization occurs, and thus ensures good control of the film deposition process on the substrate. The most used polymer in PDA is polyethyleneimine (PEI), which is a water soluble polymer with functional amino groups that coordinate the metal cations and prevent their hydrolysis [16,19]. In order to bind with PEI, metal ions are protected with chelating agent, usually ethylenediamine tetra acetic acid (EDTA). With desired ratio of PEI and EDTA it is possible to control the viscosity of the solution, optimal for deposition [17,19].

In this work bilayer structures, composed of ferromagnetic manganite and ferroelectric titanate layers, were obtained by solution deposition technique. Water-based polymer assisted deposition (PAD) was used for preparation of the first manganite layer. For the deposition of the second titanate layer, sol-gel method was used, since there is very limited choice of water soluble titanium salts usually necessary for PAD process.

## II. Experimental

The first step in preparation of the bilayer thin films was deposition of manganite layer by water-based polymer assisted deposition (PAD). Two different compositions were selected:  $\text{LaMnO}_3$  (LMO) and  $\text{La}_{0.7}\text{Sr}_{0.3}\text{MnO}_3$  (LSMO), and precursors were high-purity nitrates:  $\text{La}(\text{NO}_3)_3 \cdot 6\text{H}_2\text{O}$  ( $\geq 99.0\%$ , Fluka),  $\text{Sr}(\text{NO}_3)_2$  ( $\geq 99.0\%$ , Sigma Aldrich) and  $\text{Mn}(\text{NO}_3)_2 \cdot 4\text{H}_2\text{O}$  ( $\geq 99.0\%$ , Fisher Chemical). Nitrate solutions with concentration of 0.1 M were prepared by dissolving stoichiometric amounts of nitrates in deionized water. Ethylene diamine tetra acid (EDTA) in concentration of 7 wt.% and polyethylenamine (PEI  $M_w \sim 25000$  by LC,  $M_n \sim 10000$  by GPC) in amount corresponding to mass ratio EDTA:PEI = 1:1, were added in order to stabilize the solutions. After stirring, the nitrate solutions were deposited on ultrasonically cleaned commercially available substrates, Pt/TiO<sub>2</sub>/SiO<sub>2</sub>/Si (Pt/Si) and single crystal SrTiO<sub>3</sub> (STO) with orientation (001) by spin-coating technique. The as-prepared films were thermally treated at 750 °C in order to eliminate all organic compounds and form crystalline phase and finally annealed at 850 °C for 1 h.

The second layer, BaTiO<sub>3</sub> (BTO) or Ba<sub>0.7</sub>Sr<sub>0.3</sub>TiO<sub>3</sub> (BSTO), was obtained by sol-gel method. The pre-

cursor sols were prepared by mixing BaCO<sub>3</sub> (Merck, Germany) dissolved in glacial acetic acid with tetrabutyl-orthotitanate ( $\text{Ti}(\text{OC}_4\text{H}_9)_4$ , Fluka, Switzerland) at room temperature and pH = 1. Acetic acid and 2-methoxyethanol were used as solvents, sol-concentration was adjusted at 0.25 M, while strontium acetate ( $\text{Sr}(\text{CH}_3\text{COO})_2$ ,  $\geq 99.0\%$ , Sigma Aldrich) was used as Sr-source for the preparation of BSTO sol. The titanate layer was deposited on top of the manganite film by spin-coating technique. The obtained film was thermally treated first at 750 °C, in order to eliminate all organic compounds and form crystalline phase, and finally annealed at 850 °C for 1 h.

X-ray diffraction analyses of the investigated thin films were performed on a Rigaku, MiniFlex 600 instrument, using Ni-filtered  $\text{CuK}\alpha$  radiation in range  $2\theta = 20\text{--}60^\circ$ . Information about the structure, film growth and thickness were obtained by using transmission electron microscopy (HR-TEM, FEI Talos F200X) and high-resolution scanning electron microscopy (HR-SEM, ThermoFisher Scientific Apreo C).

## III. Results and discussion

XRD spectrum of the LMO film formed on conductive Pt/Si-type substrate is shown in Fig. 1 (blue pattern). It is obvious that the film deposited on the Pt-surface of commercial Pt/Si-type substrate has typical polycrystalline structure. All diffraction peaks belong to single-phase pseudocubic  $\text{LaMnO}_3$  phase. It is also important to underline that the LMO film has uniform structure, a very good adhesion to the substrate surface and thickness of about 10 nm [20].

### 3.1. Bilayer films on Pt/Si-type substrate

XRD spectrum of the bilayer LMO/BTO structure formed on Pt/Si-type substrate is shown in Fig. 1 (red pattern). The presence of perovskite BTO phase is confirmed with the existence of a several XRD peaks at around 22.2°, 31.7°, 46.0° and 56.5°. Even though peaks

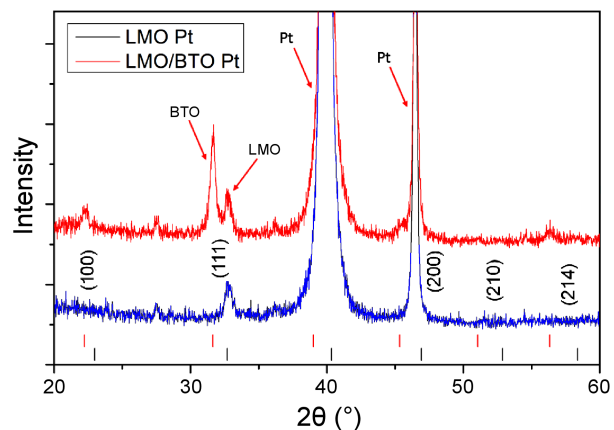


Figure 1. XRD spectra of LMO and LMO/BTO films deposited on Pt/Si-type substrates and heat treated at 850 °C

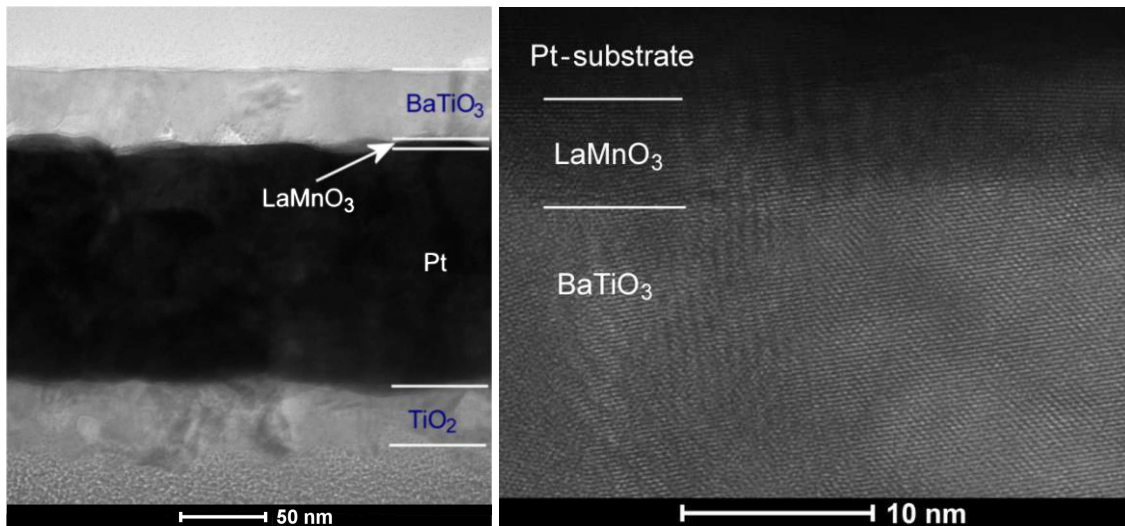


Figure 2. TEM image of LMO/BTO film deposited on Pt/Si-type substrate heated at 850 °C

of BTO phase are dominant, characteristic peak around  $\sim 32.8^\circ$  confirmed presence of LMO phase. However, a peak at  $2\theta \sim 27^\circ$  can also be observed indicating on a small portion of an impurity phase. Higher intensity of the BTO peaks can indicate difference in thickness of deposited ferromagnetic and ferroelectric layer (Fig. 2).

For good multiferroic properties at room temperature it is necessary to design bilayer structure with doped manganite layer, since it is well-known that Sr-doped LMO structure is ferromagnetic at room temperature for  $\text{Sr}^{2+}$  content between 20 and 50 at.% [21]. Thus, for the further experiments  $\text{La}_{0.7}\text{Sr}_{0.3}\text{MnO}_3$  (LSMO) was selected as a composition of manganite layer. In addition, in order to reduce mismatch between LSMO and BTO lattices, Sr ions were also added as a dopant on A-site of perovskite BTO structure and composition of the upper layer was  $\text{Ba}_{0.7}\text{Sr}_{0.3}\text{TiO}_3$  (BSTO). XRD pattern of the doped LSMO/BSTO film deposited on Pt/Si-type substrate is given in Fig. 3. Polycrystalline nature and the characteristic XRD peaks of LSMO, BSTO and Pt

phases can be recognized. The addition of Sr shifts the characteristic peaks to the higher  $2\theta$  angles as expected. Thus, the peaks at  $31.69^\circ$  and  $22.16^\circ$  for the pure BTO are moved to  $31.96^\circ$  and  $22.45^\circ$  in the doped-films, respectively. Having in mind that ionic radius of  $\text{Sr}^{2+}$  in the 12-fold coordination is smaller than ionic radius of  $\text{Ba}^{2+}$ , this shifting confirmed that  $\text{Sr}^{2+}$  entered the BTO structure. The multiple effects of Sr added to LMO film were explained in our previous paper [20].

### 3.2. Bilayer films on STO-substrate

Fast developments in nanoelectronic and spintronic devices require fabrication of highly pure, ultra-thin and epitaxial films, which forced us to modify the used solution deposition technique. In our previous paper [20] it was confirmed that the epitaxial LMO thin film can be fabricated by polymer assisted deposition (PAD) technique on the single crystal substrates. Thus, in the further experiments, instead of conductive Pt/Si-type substrate, single crystal  $\text{SrTiO}_3$  with (001) orientation was used. In Fig. 4 XRD patterns of LMO films deposited on

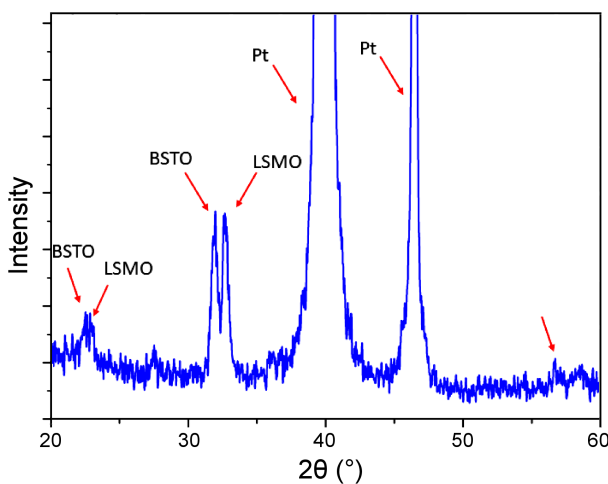


Figure 3. XRD pattern of bilayer LSMO/BSTO film deposited on Pt/Si-type substrate heated at 850 °C

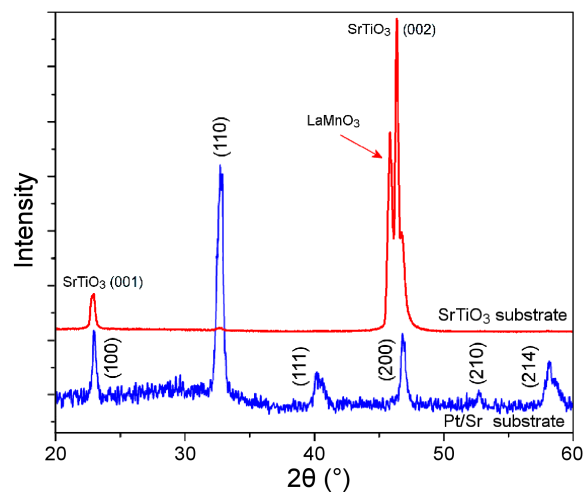


Figure 4. XRD patterns of LMO film deposited on Pt/Si and STO substrates heated at 800 °C

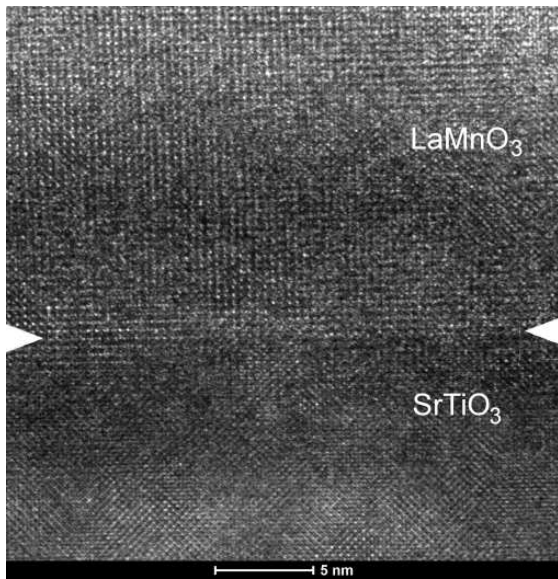


Figure 5. HR-TEM image of LMO thin film deposited on STO (001) substrate heated at 850 °C

the single crystal Si and STO substrates are compared. In contrast to the polycrystalline LMO film structure obtained on Pt/Si-type substrate, presence of the intense XRD peaks belonging to [00 $\bar{1}$ ] directions of LMO phase indicates highly oriented growth in the LMO films deposited on STO (001) substrate. The reason is similar lattice parameters of SrTiO<sub>3</sub> (which has a cubic structure with  $a = 3.905 \text{ \AA}$ ) and LaMnO<sub>3</sub> (due to simplicity it can be defined as pseudocubic with  $a = 3.95 \text{ \AA}$ ) phases [20].

The highly oriented growth can be also recognized in HR-TEM image of the LMO film on the STO (001) substrate (Fig. 5). Similar structure was obtained when PAD technique was used for the deposition of doped LSMO film on STO (001) substrate [22] with high uniformity, a very good adhesion to the substrate surface and thickness of about 10 nm.

XRD of the bilayer multiferroic film, having ferroelectric BSTO on the top of ferromagnetic LSMO layer,

deposited on the single crystal STO (001) substrate is shown in Fig. 6. It is important to underline that all three phases have relative close lattice parameters. XRD peaks originating only from (001) crystal planes are observed, which indicates the orientation of both LSMO and BSTO films in that direction. Careful analysis of the selected  $2\theta$  range of the single-layer LSMO and double-layer LSMO/BSTO films on STO (001) substrate (Fig. 6b) confirms the presence of XRD peak originating from the Ba<sub>0.7</sub>Sr<sub>0.3</sub>TiO<sub>3</sub> phase, in addition to the peaks related to the STO substrate and La<sub>0.7</sub>Sr<sub>0.3</sub>MnO<sub>3</sub> layer in the bilayer LSMO/BSTO film. The most intense peak belongs to substrate, the second one on the left side matches the LSMO phase while asymmetry pointed in the bottom of the peaks belongs to BSTO (Fig. 6b).

Thus, it can be concluded that the epitaxial growth of the LSMO film on the surface of STO substrate and the epitaxial growth of the BSTO film on the surface of LSMO/STO structure was obtained.

HR-SEM image of the bilayer LSMO/BSTO structure is given in Fig. 7. Thickness of the bilayer structure is about 100 nm, but it is not possible to see the difference between the LSMO and BSTO layers. However, uniform thickness and a very good adhesion to the STO substrate are clearly visible.

#### IV. Conclusions

In this work bilayer structures, composed of ferromagnetic manganite and ferroelectric titanate layers, were obtained by solution deposition technique, i.e. combination of polymer assisted deposition and sol-gel method. Polycrystalline structures were obtained when bilayer LaMnO<sub>3</sub>/BaTiO<sub>3</sub> and La<sub>0.7</sub>Sr<sub>0.3</sub>MnO<sub>3</sub>/Ba<sub>0.7</sub>Sr<sub>0.3</sub>TiO<sub>3</sub> films were deposited by spin coating on commercial Pt/TiO<sub>2</sub>/SiO<sub>2</sub>/Si type substrate. Thicknesses of the manganite and titanate layers were about 10 and 50 nm, respectively. However, epitaxial heterostructured films were fabricated on the single crystal SrTiO<sub>3</sub> with orientation (001). Thus, due to the similar lattice parameters of the LSMO and BSTO

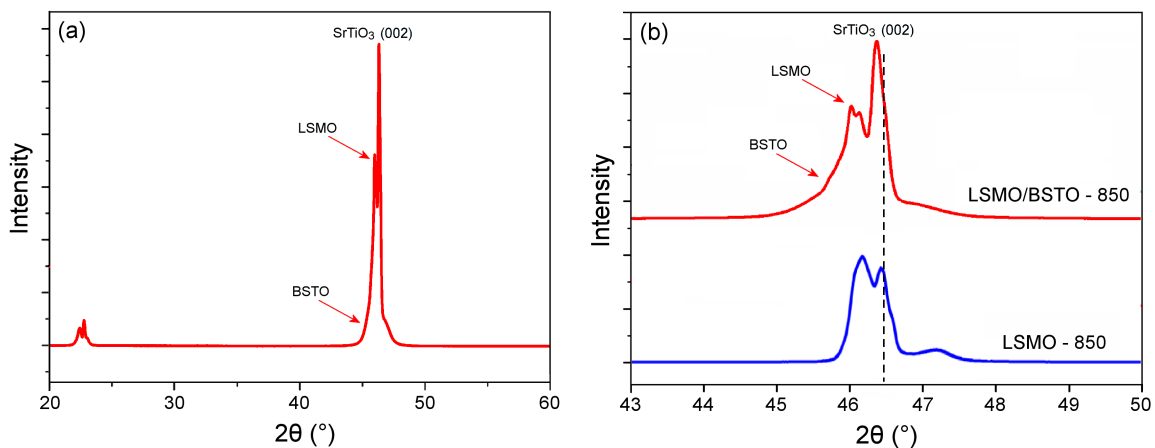
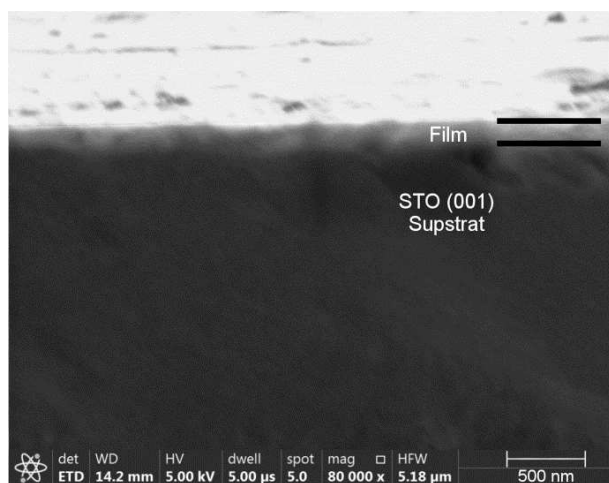


Figure 6. XRD spectrum of epitaxial LSMO/BSTO bilayer films deposited on STO (001) substrate (a) and selected  $2\theta$  range of the single-layer LSMO and double-layer LSMO/BSTO films on STO (001) substrate (b) all heated at 850 °C



**Figure 7.** HR-SEM image of LSMO/BSTO films deposited on STO (001) substrate and heated at 850 °C

phases, the  $\text{La}_{0.7}\text{Sr}_{0.3}\text{MnO}_3$  film epitaxially grown on the surface of  $\text{SrTiO}_3$  substrate followed by the epitaxial growth of the  $\text{Ba}_{0.7}\text{Sr}_{0.3}\text{TiO}_3$  film on the  $\text{La}_{0.7}\text{Sr}_{0.3}\text{MnO}_3$  surface were obtained.

**Acknowledgments:** The authors gratefully acknowledge the financial support provided by the Serbian Academy for Science and Arts, project F-137, the Ministry of Science of the Republic of Serbia, project 451-03-68/2022-14/200134 and COST Project CA17123. In addition, the authors would also like to acknowledge the help of Dr. Vladimir Rajic from the Vinca Institute of Nuclear Sciences, Serbia, for the preparation of TEM samples.

## References

1. W. Eerenstein, M. Wiora, J.L. Prieto, J.F. Scott, N.D. Mathur, "Giant sharp and persistent converse magnetoelectric effects in multiferroic epitaxial heterostructures", *Nature Mater.*, **6** (2007) 348.
2. J. Ma, J. Hu, Z. Li C.-W. Nan, "Recent progress in multiferroic magnetoelectric composites: From bulk to thin films", *Adv. Mater.*, **23** (2011) 1062–1087.
3. V.V. Srdjić, B. Bajac, M. Vijatović Petrović, M. Milanović, Ž. Cvejić, B.D. Stojanović, "Multiferroic  $\text{BaTiO}_3$ - $\text{NiFe}_2\text{O}_4$  composites: From bulk to multilayer thin films", pp. 183–219 in *Fascinating World of Nanosciences and Nanotechnologies*, Eds: V.R. Radmilović, J.Th.M. Dehossion, Serbian Academy of Sciences and Arts, Serbia, 2020.
4. I. Fina, N. Dix, J.M. Rebled, P. Gemeiner, X. Marti, F. Peiro, B. Dkhil, F. Sánchez, L. Fabrega, J. Fontcuberta, "The direct magnetoelectric effect in ferroelectric-ferromagnetic epitaxial heterostructures", *Nanoscale*, **5** (2013) 8037–8044.
5. Y. Yin, Q. Li, "A review on all-perovskite multiferroic tunnel junctions", *J. Materiomics*, **3** (2017) 245–254
6. D. Bossini, V.I. Belotelov, A.K. Zvezdin, A.N. Kalish, A.V. Kimel, "Magnetoplasmonics and femtosecond optomagnetism at the nanoscale", *ACS Photonics*, **3** (2016) 1385–1400.
7. Y.-K. Liu, Y.-W. Yin, X.-G. Li, "Colossal magnetoresistance in manganites and related prototype devices", *Chin. Phys. B*, **22** (2013) 087502.
8. W. Prellier, P. Lecoeur, B. Mercey, "Colossal magnetoresistive manganite thin films", *J. Phys.: Condens. Matter*, **13** (2001) R915–R944.
9. F.Y. Bruno, J. Garcia-Barriocanal, M. Varela, N.M. Nemes, P. Thakur, J.C. Cezar, N.B. Brookes, A. Rivera-Calzada, M. Garcia-Hernandez, C. Leon, S. Okamoto, S.J. Pennycook, J. Santamaria, "Electronic and magnetic reconstructions in  $\text{La}_{0.7}\text{Sr}_{0.3}\text{MnO}_3/\text{SrTiO}_3$  heterostructures: A case of enhanced interlayer coupling controlled by the interface", *Phys. Rev. Lett.*, **106** (2011) 147205.
10. Y.M. Sheu, S.A. Trugman, L. Yan, C.-P. Chuu, Z. Bi, Q. X. Jia, A.J. Taylor, R.P. Prasankumar, "Photoinduced stabilization and enhancement of the ferroelectric polarization in  $\text{Ba}_{0.1}\text{Sr}_{0.9}\text{TiO}_3/\text{La}_{0.7}\text{Ca}(\text{Sr})_{0.3}\text{MnO}_3$  thin film heterostructures", *Phys. Rev. B*, **88** (2013) 020101(R).
11. T. Yu, P. Chen, L. Zhou, X. Ning, B. Deng, X. Shi, H. He, "Cluster glass induced unconventional exchange bias in epitaxial  $\text{LaMnO}_3/\text{SrMnO}_3$  bilayers", *Mater. Lett.*, **242** (2019) 95–98.
12. H. Pei, Y. Zhang, S. Guo, L. Ren, H. Yan, B. Luo, C.-L. Chen, K. Jin, "Orientation-dependent optical magnetoelectric effect in patterned  $\text{BaTiO}_3/\text{La}_{0.67}\text{Sr}_{0.33}\text{MnO}_3$  heterostructures", *ACS Appl. Mater. Interfaces*, **10** [36] (2018) 30895–30900.
13. B. Nafradi, P. Szirmai, M. Spina, A. Pisoni, X. Mettan, N.M. Nemes, L. Forro, E. Horvath, "Tuning ferromagnetism at room temperature by visible light", *PNAS*, **117** [12] (2020) 6417–6423.
14. S.N. Ogugua, O.M. Ntwaeaborwa, H.C. Swart, "Latest development on pulsed laser deposited thin films for advanced luminescence applications", *Coatings*, **10** (2020) 1078.
15. A.K. Burrell, T.M. McCleskey, Q. Jia, "Polymer-assisted deposition, in *Chemical Solution Deposition of Functional Oxide Thin Films* Eds. T. Schneller, R. Waser, M. Kosec, D. Payne, Springer, Vienna, 2013
16. Q.X. Jia, T.M. McCleskey, A.K. Burrell, Y. Lin, G. Collis, H. Wang, A.D.Q. Li, S.R. Foltyn, "Polymer-assisted deposition of metal-oxide films", *Nat. Mater.*, **3** (2004) 529.
17. T.M. McCleskey, P. Shi, E. Bauer, M.J. Highland, J.A. Eastman, Z.X. Bi, P.H. Fuoss, P.M. Baldo, W. Ren, B.L. Scott, A.K. Burrell, Q.X. Jia, "Nucleation and growth of epitaxial metal-oxide films based on polymer-assisted deposition", *Chem. Soc. Rev.*, **43** (2014) 2141–2146.
18. J.M. Vila-Fungueirino, B. Rivas-Murias, J. Rubio-Zuazo, A. Carretero-Genievrier, M. Lazzari, F. Rivadulla, "Polymer assisted deposition of epitaxial oxide thin films", *J. Mater. Chem. C*, **6** (2018) 3834–3844.
19. D. Bossini, D.M. Juraschek, R.M. Geilhufe, N. Nagaosa, A.V. Balatsky, M. Milanović, V. Srdjić, P. Šenjug, E. Topić, D. Barišić, M. Rubčić, D. Pajić, Takahisa Arima, M. Savoini, S.L. Johnson, C. Davies, A. Kirilyuk, "Magnetoelectrics and Multiferroics: Theory, Synthesis, Characterisation, Preliminary Results and Perspectives for All-Optical Manipulations", *J. Phys. D: Appl. Phys.*, **56** (2023) 273001.
20. J. Vukmirovic, S. Joksovic, D. Piper, A. Nesterovic, M. Novakovic, S. Rakic, M. Milanovic, V.V. Srdic, "Epitaxial growth of  $\text{LaMnO}_3$  thin films on different single crystal substrates by polymer assisted deposition", *Ceram. Int.*, **49** (2023) 2366–2372.
21. J. Hemberger, A. Krimmel, T. Kurz, H.-A. Krug von Nidda, V.Yu. Ivanov, A.A. Mukhin, A.M. Balbashov, A.

- Loidl, “Structural, magnetic, and electrical properties of single-crystalline  $\text{La}_{1-x}\text{Sr}_x\text{MnO}_3$  ( $0.4 < x < 0.85$ )”, *Phys. Rev. B*, **66** (2002) 094410.
22. J. Vukmirović, D. Piper, P. Šenjug, D. Pajić, M. Milanović, S. Joksović, S. Rakić, M. Novaković, V.V. Srdić, “Effect of Sr-doping on structure and magnetic properties of epitaxial  $\text{LaMnO}_3$  thin films deposited by polymer assisted deposition”, *Ceram. Int.*, submitted (2023).